Design and synthesis of clathrate LaB$_8$ with superconductivity

Liang Ma,[1,2,3,*] Xin Yang,[1,2,*] Guangtao Liu,[2,*] Hanyu Liu,[2,3,4] Guochun Yang,[5,6] Hui Wang,[7] Jinqun Cai,[1,2]
Mi Zhou,[2,†] and Hongbo Wang ●[1,2,‡]

[1]*State Key Laboratory of Superhard Materials, College of Physics, Jilin University, Changchun 130012, China*
[2]*International Center of Computational Method & Software, College of Physics, Jilin University, Changchun 130012, China*
[3]*International Center of Future Science, Jilin University, Changchun 130012, China*
[4]*State Key Laboratory of Superhard Materials and Key Laboratory of Physics and Technology for Advanced Batteries (Ministry of Education), College of Physics, Jilin University, Changchun 130012, China*
[5]*Centre for Advanced Optoelectronic Functional Materials Research and Key Laboratory for UV Light-Emitting Materials and Technology of Ministry of Education, Northeast Normal University, Changchun 130024, China*
[6]*State Key Laboratory of Metastable Materials Science & Technology and Key Laboratory for Microstructural Material Physics of Hebei Province, School of Science, Yanshan University, Qinhuangdao 066004, China*
[7]*Key Laboratory for Photonic and Electronic Bandgap Materials (Ministry of Education), School of Physics and Electronic Engineering, Harbin Normal University, Harbin 150025, China*

Boron-based clathrate materials, typically with three-dimensional networks of B atoms, have tunable properties through the substitution of guest atoms, but the tuning of B cages themselves has not yet been developed. By combining a crystal structural search with the laser-heated diamond anvil cell technique, we successfully synthesized a new B-based clathrate boride, LaB$_8$, at ~108 GPa and ~2100 K. The novel structure has a B-richest cage, with 26 B atoms encapsulating a single La atom. LaB$_8$ demonstrates phonon-mediated superconductivity with an estimated transition temperature of 14 K at ambient pressure, mainly originating from the electron-phonon coupling of B cage. The replacement of La with alkaline earth metals can remarkably elevate the transition temperature. This work creates a prototype platform for subsequent investigation on tunable electronic properties through the choice of captured atoms.

I. INTRODUCTION

Elemental B exhibits extraordinary structural and chemical complexity due to different arrangements of icosahedral B$_{12}$ cages with three-center bonds within icosahedra and covalent two- and three-center bonds between icosahedra [1–3]. Through metal doping, a more B-rich B$_{24}$ cage can be obtained in a B-based clathrate metal (M) dodecaboride, MB$_{12}$, which has broadly tunable properties with different guest atoms [4–6]. To date, B-based clathrate structures have existed only in two types of MB$_{12}$ compounds, namely *I*4/*mmm* ScB$_{12}$ and *Fm*-3*m* UB$_{12}$, which include sodalite-like B$_{24}$ cages with metal atoms at the center of each B cage [4]. With different guest atoms, MB$_{12}$ exhibits properties such as superhardness (above 40 GPa for ZrB$_{12}$ [5] and Zr$_{0.5}$Y$_{0.5}$B$_{12}$ [6]), superconductivity (at 4.7 K for YB$_{12}$ and 5.8 K for ZrB$_{12}$ [7]), and oxidation resistance (at ~695°C for Y$_{0.5}$Sc$_{0.5}$B$_{12}$ [8]), making them of broad interest for industrial application. Studies of B-based clathrate materials seem to have focused mainly on guest-atom substitution [6,9]. However, the host cage may also play a vital role in determining material properties, for example, YH$_6$ with H$_{24}$ cages and YH$_9$ with H$_{28}$ cages (the recently high-pressure synthesized clathrate superhydrides) having superconductivity at 227 K [10,11] and 243 K [11,12], respectively, which are closely related to the high H-derived electron density of states at the Fermi level. The development of clathrate boride containing new B cages will create exciting opportunities for material innovation.

In classical clathrate structures, a suitable metal atomic radius is the primary requirement for accommodation in sodalite B$_{24}$ cages, with Y and Zr, respectively, being the largest and smallest metals possible [4]. Any slight size deviation renders the B-based clathrate structure unstable at ambient pressure [13]. Under high pressure, however, the chemical bonding and atomic radius are tuned, leading to synthesis of such as HfB$_{12}$, ThB$_{12}$, and GdB$_{12}$ that do not exist under ambient conditions [14,15]. Among the known MB$_{12}$ structures, Th has the largest atomic radius [16]. Considering the sensitivity of clathrate stability to the radius of guest metal atom, formation of such a clathrate structure is inhibited when the atomic radius of the candidate metal atom differs significantly from that of existing clathrate borides. Furthermore, the formation of such a clathrate structure is associated with electron transfer from metal to the B atom. Based on these factors, La may be a suitable metal candidate, with a slightly larger atomic radius and lower electronegativity than those of Th [16,17], which means that it might react with B at high pressures to form a novel clathrate structure.

The formation of La-B compounds under ambient pressures has been extensively studied, but only LaB_4 and LaB_6 phases have been characterized reliably [18,19]. Their structures feature three-dimensional B backbones of B_6 octahedra with La in interstitial sites. The LaB phase, comprising graphite-like B^- layers, becomes stable above 30 GPa [20]. The behavior of La-B compounds at higher pressures remains relatively unexplored. Here we experimentally and theoretically investigate the chemistry of the binary La-B system at high pressures, finding a series La-B compounds thermodynamically stable at high pressure. A novel clathrate LaB_8 compound with B_{26} cages was discovered under high-pressure conditions. Electronic property calculations indicate its metallic character with a superconducting transition temperature T_c of 14 K at ambient pressure. LaB_8 exhibits tunable properties, with marked enhancement of T_c through substitution of alkaline earth metals for La.

II. METHODS

Structure prediction of the lanthanum borides were performed by using a swarm intelligence structure search method, as implemented in the CALYPSO code [21,22], which has been validated with various known compounds [23–25]. We performed a structure prediction employing simulation cells with 1, 2, and 4 formula units (f.u.) at selected pressures of 1 atm and 50, 100, and 150 GPa. The *ab initio* structural relaxations and electronic property calculations were performed in the framework of density functional theory [26,27] within the generalized gradient approximation (GGA) [28] and frozen-core all-electron projector-augmented wave (PAW) method [29,30], as implemented in the VASP code [31–33], where $5s^2 5p^6 6s^2 5d^1$ and $2s^2 2p^1$ electrons were taken as the valence electrons for La and B atoms, respectively. A plane-wave kinetic energy cutoff of 650 eV and appropriate Monkhorst-Pack k-meshes with grid spacing of $2\pi \times 0.03\,\text{Å}^{-1}$ were chosen to ensure that enthalpy calculations were converged to less than 1 meV/atom. The phonon calculations were carried out using both finite displacement approach through the PHONOPY code [34]. The electron-phonon coupling calculations were carried out using QUANTUM-ESPRESSO (QE) package [35]. Ultrasoft pseudopotentials were used with a kinetic energy cutoff of 50 Ry. Bader's quantum theory of atoms in molecules (QTAIM) analysis was employed for the charge transfer calculation [36].

Lanthanum metal (Alfa Aesar 99.5%), LaB_6 (Alfa Aesar 99.5%) and B (Alfa Aesar, 99.99%) were purchased commercially and used without further purification. In the cell-1, La foil with the thickness of $2\,\mu m$ was sandwiched between the B plate ($\sim 10\,\mu m$) and MgO plate ($\sim 1\,\mu m$). While in cell-2 and cell-3, binary (LaB_6 + B) mixtures were milled using Si_3N_4 media at 600 rpm for 1-min cycles over ~ 24 hours. The milled powders were pressed to thin plates ($10\,\mu m$) then loaded into DAC sample chambers. The diamonds used in DACs had culets with diameter of 60-150 μm and were beveled at $8.5°$ to a diameter of about $250\,\mu m$. A composite gasket consisting of a rhenium outer annulus and a cubic boron nitride (c-BN) epoxy mixture insert was employed, and MgO plates served as thermal insulation from diamond anvils. The sample preparations were done in a glovebox with an
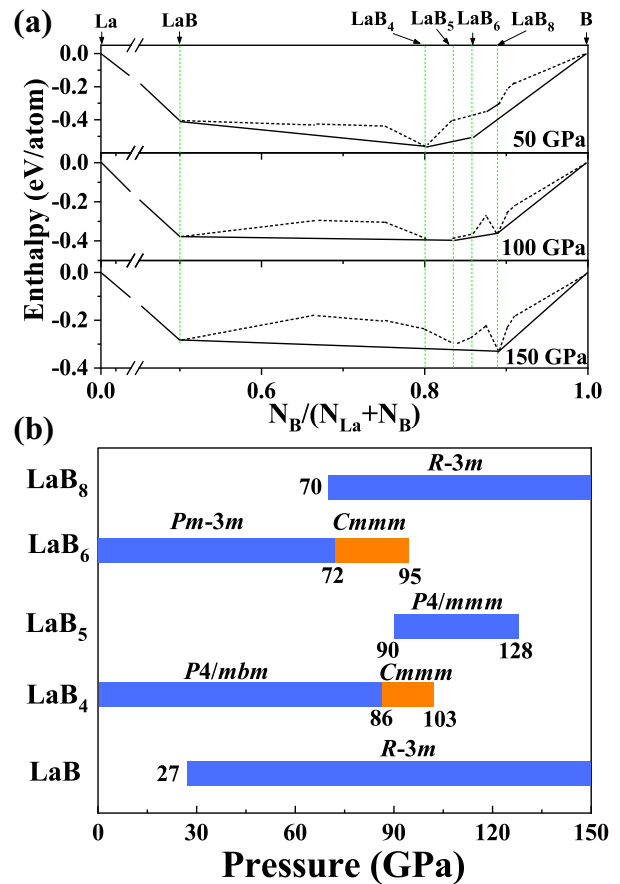

FIG. 1. (a) Thermodynamic stability of various La-B compounds with respect to elements La and B at selected pressures. The energetically stable phases are shown using solid symbols connected by solid lines on the convex hull. (b) Pressure-composition phase stability diagram of the La-B system.

inert Ar atmosphere and the contents of O_2 and H_2O less than 0.01 ppm. After being compressed to the certain pressure at room temperature, samples were heated to about 2100 K with a one-sided pulsed radiation from a YAG laser. The pressure values were determined from Raman spectra of diamond [37] and the equation of state (EOS) of the contacted MgO plate [38].

In situ high-pressure x-ray diffraction measurements were performed at beamline BL15U1 (0.6199 Å) of the Shanghai Synchrotron Radiation Facility and HP-Station 4W2 of the Beijing Synchrotron Radiation Facility. Using the geometric parameters calibrated by a CeO_2 standard, the DIOPTAS software package was used to integrate the powder diffraction patterns then convert to one-dimensional profiles [39]. Rietveld refinements of XRD patterns were conducted using GSAS with EXPGUI packages [40]. Additionally, the dependencies of the volume on pressure were fitted by the third-order Birch-Murnaghan equation [41] to determine the main parameters of the EOS.

III. RESULTS AND DISCUSSION

In seeking a new type of B-based clathrate we undertook an extensive search of known structures based on
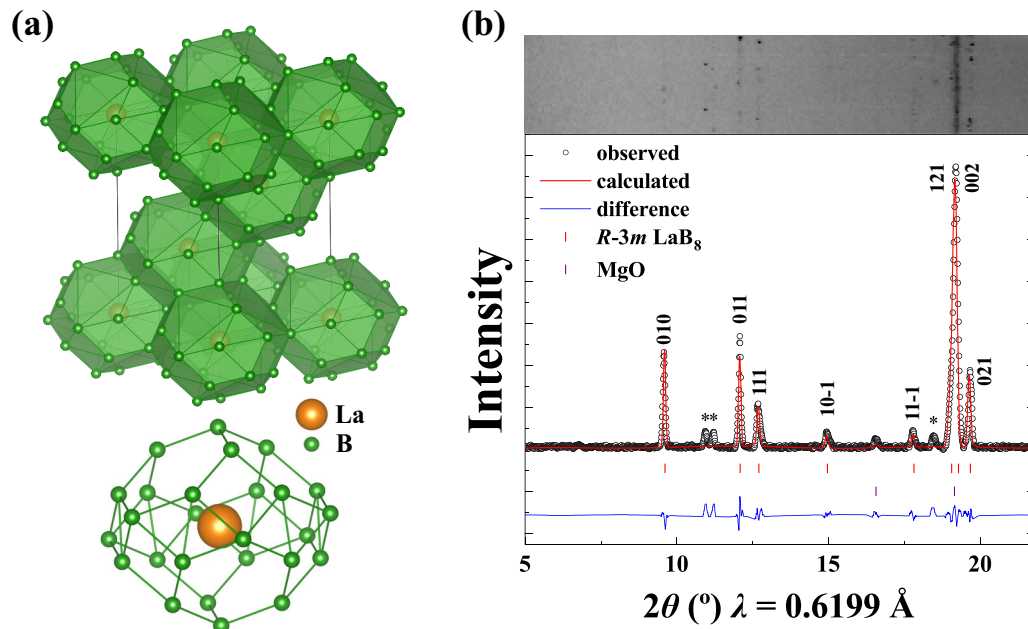
FIG. 2. (a) The crystal structures of clathrate LaB$_8$. Each cage consists of 12 twisted rhombi and six twisted hexagons, with a single La atom at the center. (b) Experimental XRD data (black points) of cell-3 collected at 131 GPa with Rietveld refinement (red line) of the *R*-3*m* LaB$_8$ and *Fm*-3*m* MgO phase. The two-dimensional cake image is presented above the integrated pattern. Unidentified reflections are indicated by asterisks.

stoichiometric LaB$_x$ ($x = 1$–10) at pressures of 50, 100, and 150 GPa (Fig. 1). The energetic stabilities of LaB$_x$ compounds were evaluated from their formation enthalpies with respect to the dissociation products of La [42] and B [1] solids. Previously known LaB, LaB$_4$, and LaB$_6$ phases were readily identified [18–20], indicating the reliability of our calculations [Fig. 1(b)]. The high-pressure phases of LaB$_4$ and LaB$_6$, both with a *Cmmm* space group (Fig. S1 [43]), and two unexpected compositions of LaB$_5$ and LaB$_8$ become stable at elevated pressures. Detailed structural information, electronic properties, and phonon dispersion curves are shown in Figs. S2 to S4 and Table S1 [43].

Interestingly, LaB$_8$ exhibits peculiar three-dimensional B clathrate structures comprising contiguous face-sharing B$_{26}$ cages [Fig. 2(a)] in which single La atoms are nested. These cages are constructed from 12 twisted rhombi and 6 twisted hexagons, with B–B bond lengths of 1.65–1.72 Å at 100 GPa. Enthalpy calculations reveal its thermodynamic stability above 70 GPa. LaB$_8$ appears to be an unprecedented stoichiometry in metal borides that contain more B-rich cages than conventional B$_{24}$ cages in clathrate MB$_{12}$. In phonon calculations, clathrate LaB$_8$ exhibits no imaginary phonon frequencies at 0–150 GPa (Fig. S4 [43]), indicating its dynamical stability. The electron localization function (ELF) and Bader charge analysis were undertaken to explore the bonding nature of the clathrate structure LaB$_8$ (Fig. S5 and Table S3 [43]). Results indicate strong covalent bonding between B atoms and weak ionic bonding between La and the B$_{26}$ cage. Because of the strong B–B covalent bonding, we investigated the specific Vickers hardness (H_v) of *R*-3*m* LaB$_8$ using an empirical model [44]. The calculated hardness of *R*-3*m* LaB$_8$ is 25.3 GPa, indicating the possibility of its being a hard material.

Guided by theoretical prediction, we carried out laser-heated diamond anvil cell (LHDAC) experiments to synthesize the target clathrate LaB$_8$. In cell-1, a piece of La foil and excess B powder were compressed to 115 GPa and heated to ∼2100 K. X-ray diffraction (XRD) patterns (Fig. S6(a) [43]) indicate a complex mixture of products with predominant LaB$_8$ marked by a red bar below the pattern. There were also some unidentified Bragg peaks.

To obtain high-quality XRD patterns of clathrate LaB$_8$, homogeneous fine-grained mixtures of LaB$_6$ and B were used as precursors in cell-2 and cell-3 experiments, targeting the stoichiometric reaction, LaB$_6$ + 2B → LaB$_8$. Samples were compressed to 108 GPa and 131 GPa, respectively, then laser heated to ∼2100 K. XRD patterns (Figs. 2(b) and S7 [43]) are consistent with the patterns calculated for clathrate LaB$_8$. The peaks marked with asterisks in Fig. 2(b) could not be reproduced in other experiments, indicating that they may be due to other LaB stochiometries or impurities. Upon decompression, LaB$_8$ was stable to at least 83 GPa, decomposing to LaB$_6$ and B at 66 GPa [Fig. 3(a)]. Due to the relatively low atomic scattering power of B, the diffraction patterns are mainly determined by La sublattice. Therefore, we further developed the EOS fitted in the unloading process, which is highly consistent with the theoretical EOS of LaB$_8$, demonstrating that we successfully synthesized clathrate LaB$_8$. Considering that the LaB$_8$ structure is dynamically stable at atmospheric pressure, one may therefore be stabilized via some special techniques, such as releasing pressure at low temperature [45,46], rapid pressure-quenching method [47–49], and so on.

The discovery of superconductivity in MgB$_2$ at 39 K [50] provided a new perspective in the search for metal boride materials with high T_c, with strong electron-phonon coupling
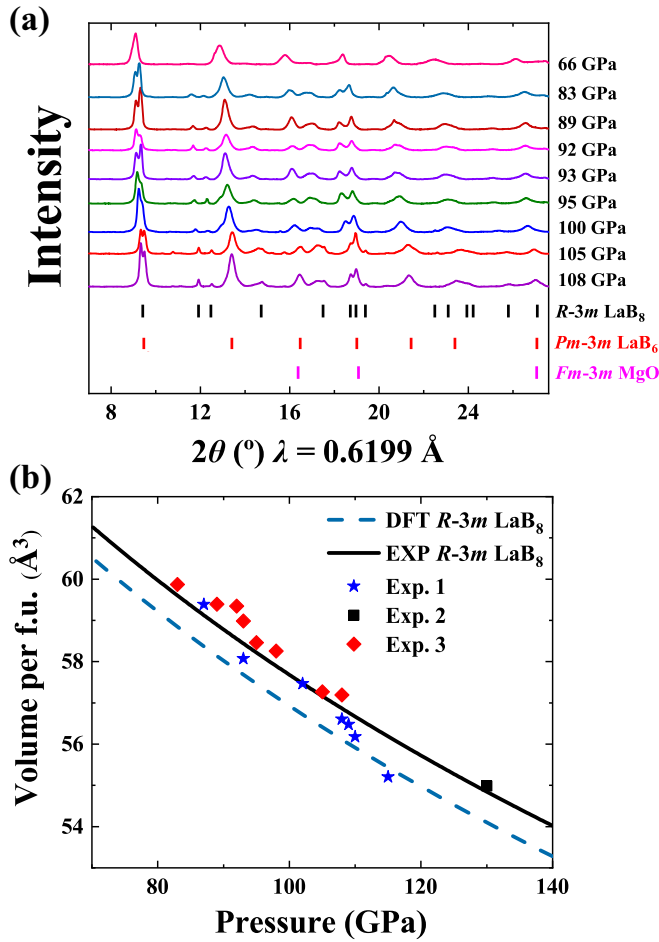
(a)

(b)

FIG. 3. (a) Experimental XRD patterns of cell-2 during decompression in the pressure range of 66–108 GPa. (b) Experimental EOS (solid black line) with $B_0 = 194(2)$ GPa, $B'_0 = 4.0$ (fixed) and calculated EOS (dashed lines) with $B_0 = 188(1)$ GPa (DFT-PBE), $B'_0 = 4.0$ (fixed) for R-3m LaB$_8$. Experimental data for the samples are shown as asterisk, rhombus, and square points. The third-order Birch-Murnaghan equation was fitted to the PV data.

(a)

(b)

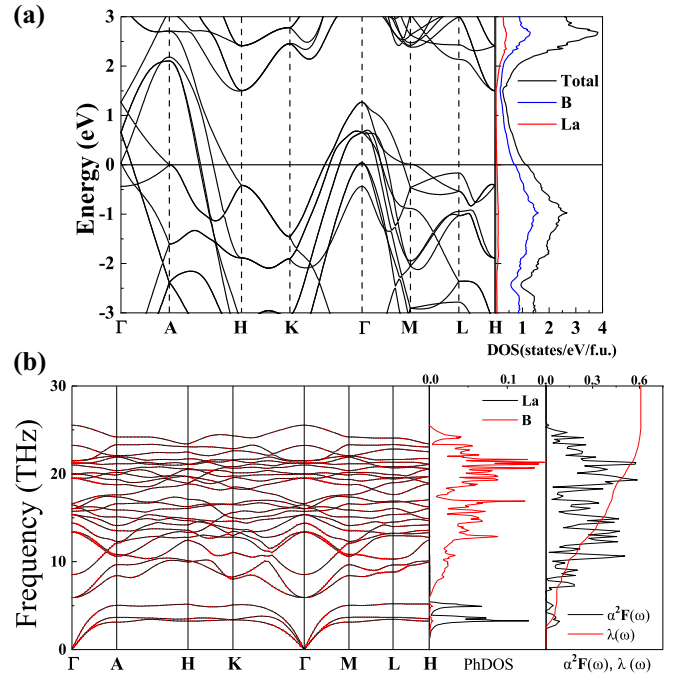
FIG. 4. (a) The electronic band structure and projected DOS for R-3m LaB$_8$ at 0 GPa. (b) Phonon dispersion relations, projected PHDOS, and Eliashberg spectral function for of LaB$_8$ at 0 GPa. The size of the red dots represents the magnitude of the EPC.

of B layers in the structure being largely responsible for the high T_c [51]. However, the rather low superconductivity of 0.39 K, 4.7 K, 5.8 K, and 0.4 K were observed in conventional clathrate borides MB$_{12}$, for ScB$_{12}$, YB$_{12}$, ZrB$_{12}$, and LuB$_{12}$, respectively [52,53]. Therefore, we are quite curious about the superconductivity in the novel clathrate boride LaB$_8$. We first performed the electronic property calculations for LaB$_8$ at selected pressures and compared the results with those for LaB$_{12}$, the structure of which was constructed from known prototype structures of $I4/mmm$ ScB$_{12}$ and Fm-3m UB$_{12}$ (Figs. 4(a) and S8 [43]). The results indicate the metallic nature of all three structures, with the B-derived DOS value of LaB$_8$ around the Fermi level (FL) being higher than that of LaB$_{12}$, which means the superconductivity may be significantly improved. The superconducting T_c value was estimated using the Allen-Dynes modified McMillan equation (Figs. 4(b) and S9 [43]). The electron-phonon coupling constant λ of LaB$_8$ is calculated to be 0.61, which is larger than that of Fm-3m LaB$_{12}$ (0.25) and $I4/mmm$ LaB$_{12}$ (0.24), leading the estimated T_c as high as 14 K at ambient pressure

with μ^* of 0.1, much higher than 0.01 K and 0.01 K in Fm-3m LaB$_{12}$ and $I4/mmm$ LaB$_{12}$.

The phonon dispersion, projected phonon DOS, and Eliashberg spectral function [$\alpha^2F(\omega)$ and its integral $\lambda(\omega)$] calculations of LaB$_8$ were all undertaken to explore the superconducting properties [Fig. 4(b)]. The calculated phonon DOS can be separated into two regions: low-frequency vibrations (0–6 THz) related to La atoms and the high-frequency vibrations related to B atoms. The vibrations of B atoms in a large range of 6–26 THz contribute as much as 89% to the total λ. Considering the significant DOS at the FL of B atoms, we therefore conclude that the coupling between the electrons and phonon vibrations of B atoms is responsible for the high superconductivity of LaB$_8$. While the average phonon frequency gradually increases with decreasing λ at higher pressures, leading to a predicted T_c of 2.1 K at 100 GPa.

The electronic DOS of LaB$_8$ exhibits a peak below the FL [Fig. 4(a)], providing a feasible means of increasing the electronic DOS around the FL through the tunable electronic structure of the B$_{26}$ cage in LaB$_8$. We substituted La of R-3m LaB$_8$ with other guest ions to construct a series of R-3m structures of MB$_8$ compounds (M = Mg, Ca, Sr, Y). Phonon dispersion relations of these structures indicate their dynamic stability at ambient pressure (Fig. S4 [43]). Electron-phonon calculations of substituted MB$_8$ were performed at ambient pressure, with specific λ, $\alpha^2F(\omega)$, and T_c values as listed in Figs. S9 and S10 [43]. With alkaline earth elements inserted into the B$_{26}$ cage there was less electron transfer to B atoms than La atom, leading to a notable increase in electron density around the FL (Fig. S10 [43]). As anticipated, the MB$_8$

(M = Mg, Ca, Sr) structures demonstrate high-temperature superconductivity at ambient pressure (Fig. S10 [43]). The current results could provide a theoretical guidance for future experiments.

IV. CONCLUSION

The high-pressure behavior of binary La-B compounds was investigated by combining a crystal structural search and the LHDAC technique. A novel clathrate boride, LaB$_8$, with a three-dimensional B network of B$_{26}$ cages with a La atom at the center, was successfully synthesized at high pressure and temperature. Electronic property calculations indicate its metallic nature with a predicted T_c of 14 K at ambient pressure. Subsequent calculations indicated its tunable properties, with T_c values showing a great improvement with substitution of alkaline earth metals for La. This study provides a new platform for the design of materials with tunable electronic properties, and may stimulate high-pressure experimental

work on the synthesis of high-T_c superconductors based on clathrate structures.

[1] A. R. Oganov, J. Chen, C. Gatti, Y. Ma, Y. Ma, C. W. Glass, Z. Liu, T. Yu, O. O. Kurakevych, and V. L. Solozhenko, Nature (London) **457**, 863 (2009).

[2] R. E. Hughes, C. H. L. Kennard, D. B. Sullenger, H. A. Weakliem, D. E. Sands, and J. L. Hoard, J. Am. Chem. Soc. **85**, 361 (1963).

[3] B. Albert and H. Hillebrecht, Angew. Chem., Int. Ed. **48**, 8640 (2009).

[4] G. Akopov, M. T. Yeung, and R. B. Kaner, Adv. Mater. **29**, 1604506 (2017).

[5] T. Ma, H. Li, X. Zheng, S. Wang, X. Wang, H. Zhao, S. Han, J. Liu, R. Zhang, P. Zhu *et al.*, Adv. Mater. **29**, 1604003 (2017).

[6] G. Akopov, W. H. Mak, D. Koumoulis, H. Yin, B. Owens-Baird, M. T. Yeung, M. H. Muni, S. Lee, I. Roh, Z. C. Sobell *et al.*, J. Am. Chem. Soc. **141**, 9047 (2019).

[7] R. Troć, R. Wawryk, A. Pikul, and N. Shitsevalova, Philos. Mag. **95**, 2343 (2015).

[8] Y. Liang, Y. Zhang, H. Jiang, L. Wu, W. Zhang, K. Heckenberger, K. Hofmann, A. Reitz, F. C. Stober, and B. Albert, Chem. Mater. **31**, 1075 (2019).

[9] J. Lei, G. Akopov, M. T. Yeung, J. Yan, R. B. Kaner, and S. H. Tolbert, Adv. Funct. Mater. **29**, 1900293 (2019).

[10] I. A. Troyan, D. V. Semenok, A. G. Kvashnin, A. V. Sadakov, O. A. Sobolevskiy, V. M. Pudalov, A. G. Ivanova, V. B. Prakapenka, E. Greenberg, A. G. Gavriliuk *et al.*, Adv. Mater. **33**, 2006832 (2021).

[11] P. Kong, V. S. Minkov, M. A. Kuzovnikov, A. P. Drozdov, S. P. Besedin, S. Mozaffari, L. Balicas, F. F. Balakirev, V. B. Prakapenka, S. Chariton *et al.*, Nat. Commun. **12**, 5075 (2021).

[12] E. Snider, N. Dasenbrock-Gammon, R. McBride, X. Wang, N. Meyers, K. V. Lawler, E. Zurek, A. Salamat, and R. P. Dias, Phys. Rev. Lett. **126**, 117003 (2021).

[13] S. La Placa, I. Binder, and B. Post, J. Inorg. Nucl. Chem. **18**, 113 (1961).

[14] J. F. Cannon and P. B. Farnsworth, J. Less-Common Met. **92**, 359 (1983).

[15] J. F. Cannon, D. M. Cannon, and H. T. Hall, J. Less-Common Met. **56**, 83 (1977).

[16] J. C. Slater, J. Chem. Phys. **41**, 3199 (1964).

[17] M. Rahm, R. Cammi, N. W. Ashcroft, and R. Hoffmann, J. Am. Chem. Soc. **141**, 10253 (2019).

[18] K. Kato, I. Kawada, C. Oshima, and S. Kawai, Acta Crystallogr., Sect. B: Struct. Crystallogr. Cryst. Chem. **30**, 2933 (1974).

[19] M. E. Schlesinger, P. K. Liao, and K. E. Spear, J. Phase Equilib. **20**, 73 (1999).

[20] A. G. Van Der Geest and A. N. Kolmogorov, Calphad **46**, 184 (2014).

[21] Y. Wang, J. Lv, L. Zhu, and Y. Ma, Phys. Rev. B **82**, 094116 (2010).

[22] Y. Wang, J. Lv, L. Zhu, and Y. Ma, Comput. Phys. Commun. **183**, 2063 (2012).

[23] X. Yang, H. Li, H. Liu, H. Wang, Y. Yao, and Y. Xie, Phys. Rev. B **101**, 184113 (2020).

[24] F. Peng, Y. Sun, C. J. Pickard, R. J. Needs, Q. Wu, and Y. Ma, Phys. Rev. Lett. **119**, 107001 (2017).

[25] L. Ma, G. Liu, Y. Wang, M. Zhou, H. Liu, F. Peng, H. Wang, and Y. Ma, arXiv:2002.09900.

[26] P. Hohenberg and W. Kohn, Phys. Rev. **136**, B864 (1964).

[27] W. Kohn and L. J. Sham, Phys. Rev. **140**, A1133 (1965).

[28] J. P. Perdew, K. Burke, and M. Ernzerhof, Phys. Rev. Lett. **77**, 3865 (1996).

[29] P. E. Blöchl, Phys. Rev. B **50**, 17953 (1994).

[30] G. Kresse and D. Joubert, Phys. Rev. B **59**, 1758 (1999).

[31] G. Kresse and J. Hafner, Phys. Rev. B **48**, 13115 (1993).

[32] G. Kresse and J. Hafner, Phys. Rev. B **49**, 14251 (1994).

[33] G. Kresse and J. Furthmüller, Comput. Mater. Sci. **6**, 15 (1996).

[34] A. Togo, F. Oba, and I. Tanaka, Phys. Rev. B **78**, 134106 (2008).

[35] P. Giannozzi, S. Baroni, N. Bonini, M. Calandra, R. Car, C. Cavazzoni, D. Ceresoli, G. L Chiarotti, M. Cococcioni, I. Dabo *et al.*, J. Phys.: Condens. Matter **21**, 395502 (2009).

[36] W. Tang, E. Sanville, and G. Henkelman, J. Phys.: Condens. Matter **21**, 084204 (2009).

[37] Y. Akahama and H. Kawamura, J. Appl. Phys. **100**, 043516 (2006).

[38] S. M. Dorfman, V. B. Prakapenka, Y. Meng, and T. S. Duffy, J. Geophys. Res.: Solid Earth **117**, B08210 (2012).

[39] C. Prescher and V. B. Prakapenka, High Pressure Res. **35**, 223 (2015).

[40] B. H. Toby, J. Appl. Crystallogr. **34**, 210 (2001).

[41] F. Birch, Phys. Rev. **71**, 809 (1947).

[42] W. Chen, D. V. Semenok, I. A. Troyan, A. G. Ivanova, X. Huang, A. R. Oganov, and T. Cui, Phys. Rev. B **102**, 134510 (2020).

[43] See Supplemental Material at http://link.aps.org/supplemental/10.1103/PhysRevB.104.174112 for full lists of structural parameters, computational details, phonon dispersion curves, projected phonon density of states (PHDOS), electronic band structures, projected density of states, and electron localization function (ELF), bader calculation, and superconducting properties of predicted stable La-B phases. High pressure x-ray diffraction data of all synthezied La-B phases.

[44] J. S. Tse, J. Super. Mater. **32**, 177 (2010).

[45] Z. Wu, L. Deng, M. Gooch, S. Huyan, and C. Chu, Mater. Today Phys. **15**, 100291 (2020).

[46] B. Trevor, L. Deng, R. Dahal, Y. Xie, B. Gao, X. Li, K. Yin, M. Gooch, D. Rolston, T. Chen *et al.*, Bulletin of the American Physical Society **J04**, J04.00006 (2021).

[47] L. Deng, T. Bontke, R. Dahal, Y. Xie, B. Gao, X. Li, K. Yin, M. Gooch, D. Rolston, T. Chen *et al.*, Proc. Natl. Acad. Sci. U S A **118**, e2108938118 (2021).

[48] Q. Sun, X. Zhao, Y. Feng, Y. Wu, Z. Zhang, X. Zhang, X. Wang, S. Feng, and X. Liu, Inorg. Chem. Front. **5**, 669 (2018).

[49] L. Zhang, Y. Wang, J. Lv, and Y. Ma, Nat. Rev. Mater. **2**, 17005 (2017).

[50] J. Nagamatsu, N. Nakagawa, T. Muranaka, Y. Zenitani, and J. Akimitsu, Nature (London) **410**, 63 (2001).

[51] J. M. An and W. E. Pickett, Phys. Rev. Lett. **86**, 4366 (2001).

[52] S. T. Matthias, T. H. Geballe, K. Andres, E. Corenzwit, G. W. Hull, and J. P. Maita, Science **159**, 530 (1968).

[53] I. Bat'ko, M. Bat'kov'a, K. Flachbart, V. B. Filippov, Y. B. Paderno, N. Y. Shitsevalova, and T. Wagner, J. Alloys Compd. **217**, L1 (1995).